Stopping Light in a Waveguide with an All-Optical Analog of Electromagnetically Induced Transparency

Mehmet Fatih Yanik, Wonjoo Suh, Zheng Wang, and Shanhui Fan*

Ginzton Laboratory, Stanford University, Stanford, California 94305, USA
(Received 9 July 2004; published 1 December 2004)

We introduce a new all-optical mechanism that can compress the bandwidth of light pulses to absolute zero, and bring them to a complete stop. The mechanism can be realized in a system consisting of a waveguide side coupled to tunable resonators, which generates a photonic band structure that represents a classical analogue of the electromagnetically induced transparency. The same system can also achieve a time-reversal operation. We demonstrate the operation of such a system by finite-difference time-domain simulations of an implementation in photonic crystals.

The ability to stop a light pulse, while completely preserving quantum coherent information encoded in the pulse, has profound implications for classical and quantum information processing [1–5]. Up to now, most experimental demonstrations of stopping light rely upon the use of electromagnetic induced transparency (EIT). In these experiments, a light pulse is stopped by completely or partially transferring the optical information to coherent electronic states [6–8]. The use of electronic states, however, severely limits applications, due to the stringent conditions required to maintain electronic coherence.

Since the EIT spectrum results from the interference of resonant pathways, it has been recently recognized that similar interference effects also occur in classical systems such as plasma and electric circuits [9,10]. In particular, EIT-like transmission spectra have been observed in static optical resonators [11–13]. To stop light, however, a static resonator system alone is not sufficient—any such resonator system is fundamentally limited by the delay-bandwidth constraint [14,15] and cannot bring the group velocity of an optical pulse to zero [5,16]. Critically, one needs to develop the correct dynamic process that allows the bandwidth of the pulse to be adiabatically compressed to zero [5,16]. Yanik and Fan recently showed one such dynamic process based upon a band anticrossing mechanism in coupled resonator optical waveguides (CROW) [5].

In this Letter, we theoretically and numerically demonstrate a new and optimal mechanism for stopping light, by constructing a classical analogue of EIT consisting of a waveguide side coupled to optical resonators, and by modulating the refractive index of the resonators to dynamically compress photon bandwidth. We prove that the group velocity of light can be reduced to absolute zero, with only two resonators per unit cell, due to the presence of EIT-like interference effects. We also show that in such a system, the adiabatic bandwidth compression process is protected by the presence of a large photonic band gap, which makes a fast compression process possible.

We consider a translationally invariant system (Fig. 1), in which a waveguide is coupled to two side cavities in each unit cell. The cavities have resonant frequencies ω_A and ω_B, respectively. Initially, we assume that the cavities couple to the waveguide with equal rates of $1/\tau$, and we ignore the direct coupling between the side cavities. The transmission matrix for a waveguide side coupled to a single resonator with resonance frequency ω_i can be calculated using the Green's function method [17] as

$$T_{c_i} = \begin{pmatrix} 1 + j/(\omega - \omega_i)\tau & j/(\omega - \omega_i)\tau \\ -j/(\omega - \omega_i)\tau & 1 - j/(\omega - \omega_i)\tau \end{pmatrix}. \quad (1)$$

The transmission matrix through an entire unit cell in Fig. 1 can then be determined as

$$T = T_{c_1} T_{l_1} T_{c_2} T_{l_2}, \quad (2)$$

where

$$T_{l_i} = \begin{pmatrix} e^{-j\beta l_i} & 0 \\ 0 & e^{j\beta l_i} \end{pmatrix}$$

is the transmission matrix for a waveguide section of length l_i. Here, β is the wave vector of the waveguide at a given frequency ω.

Since $\det(T) = 1$, the eigenvalues of T can be represented as e^{ikl}, e^{-ikl}, where $l = l_1 + l_2$ is the length of the
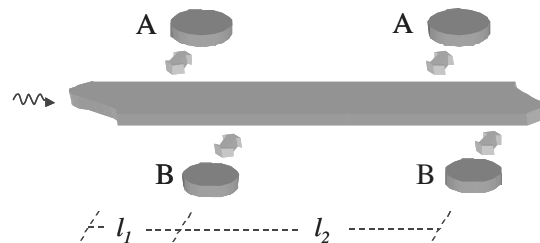

FIG. 1.   Schematic of a tunable waveguide system used to stop light. The disks and block represent the cavities and the waveguide. The arrows indicate available evanescent coupling pathways between the cavities and the waveguide. The system consists of a periodic array of two side cavities coupled to the waveguide, with a coupling rate of $1/\tau$. The distance between the nearest neighbor side cavities is l_1, and the length of the unit cell is $l = l_1 + l_2$.

233903-1

unit cell, and k (when it is real) corresponds to the Bloch wave vector of the entire system. Therefore, we obtain the band diagram of the system as

$$\frac{1}{2}\text{Tr}(T) = \cos(kl) = f(\omega)$$

$$\equiv \cos(\beta l) + \frac{C_+}{(\omega - \omega_A)} + \frac{C_-}{(\omega - \omega_B)}, \quad (3)$$

where $C_\pm = \frac{2\sin(\beta l_1)\sin(\beta l_2)}{(\omega_A - \omega_B)\tau^2} \pm \frac{\sin(\beta l)}{\tau}$. In the frequency range where $|f(\omega)| < 1$, the system supports propagating modes, while $|f(\omega)| > 1$ corresponds to the frequency ranges of the photonic band gaps. For a large frequency separation $\Delta = |\omega_A - \omega_B|\tau$, the band diagram is shown in Fig. 2(a). In the vicinity of the resonances, the system supports three photonic bands, with two gaps occurring around ω_A and ω_B. Such a band diagram is similar to that of EIT systems [18].

The width of the middle band depends strongly on the resonant frequencies ω_A, ω_B. Importantly, when the resonant frequencies satisfy the following conditions, the width of the middle band becomes zero [Fig. 2(b)], with the frequency of the entire band pinned at ω_A:

$$C_+(\omega_A) = \frac{2\sin[\beta(\omega_A)l_1]\sin[\beta(\omega_A)l_2]}{(\omega_A - \omega_B)\tau^2} + \frac{\sin[\beta(\omega_A)l]}{\tau} \to 0,$$
$$(4)$$

$$\left| \cos[\beta(\omega_A)l] + \frac{C_-(\omega_A)}{\omega_A - \omega_B} \right| > 1. \quad (5)$$

(Alternatively, the band can be pinned at ω_B with a similar condition.) To prove these conditions, we note
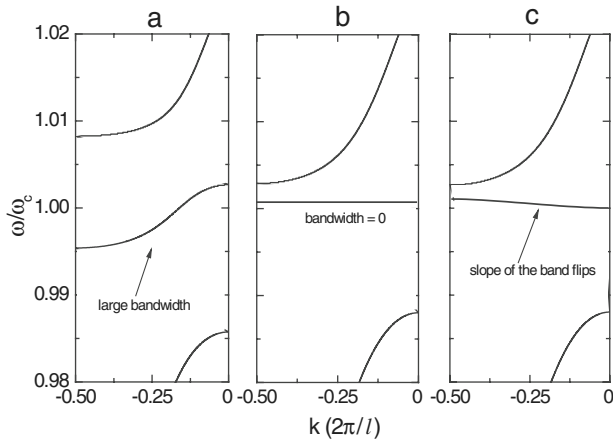

FIG. 2. The photonic bands of the system of Fig. 1 for three different choices of $\Delta \equiv |\omega_A - \omega_B|\tau$. (a) $\Delta = 3.277$. The bandwidth of the middle band is large. (b) $\Delta \approx 0.341$. The bandwidth goes to zero. (c) $\Delta = 0$. The slope of the band flips its sign. The cavity resonance frequencies are given by $\omega_{A,B} = \omega_c \mp \Delta/2\tau$ where $\omega_c = 0.357(2\pi c/a)$ and $1/\tau = \omega_c/235.8$. Here, a is a length unit. The distances between the cavities are $\ell_1 = 2a$ and $\ell = 8a$. The waveguide has a dispersion of $\beta = [0.278 + 0.327(\omega a/2\pi c - 2.382)]/a$, which is actually a fit for the photonic crystal waveguide in Fig. 3.

that $f(\omega)$ in Eq. (3) has a singularity at $\omega = \omega_A$. The frequency width of this singularity is controlled by $C_+(\omega_A)$, and approaches zero when Eq. (4) is satisfied. Satisfying Eq. (5), on the other hand, ensures that the solutions to $|f(\omega)| \le 1$ in the vicinity of ω_A occurs on the same branch of the singularity $1/(\omega - \omega_A)$, and thus forms a continuous band. When both conditions are satisfied, as the width of the singularity approaches zero, a band [the middle band in Fig. 2(b)] always exists in the vicinity of ω_A, and the width of this middle band vanishes. Upon further decrease of Δ, the group velocity of the band changes sign [Fig. 2(c)]. Furthermore, the sign of the group velocity for the middle band can be designed by choosing appropriate l_1, l_2.

In the presence of direct coupling due to photon tunneling between the two cavities in the same unit cell, one could still describe the system in terms of two resonant eigenstates within each unit cell. The dispersion can be expressed in the same functional form as of Eq. (3) with ω_A and ω_B in the denominator replaced by the frequencies of the eigenstates. And bandwidth compression to zero still occurs when conditions analogous to that of Eqs. (4) and (5) are satisfied. This is also supported by our numerical observations that the sign of the band flips. In addition, in photonic crystals, the direct coupling constant decreases exponentially with the distance between the cavities, and can therefore be reduced to any desired value in our system since the cavities are not across each other along the waveguide. Our simulations also indicate that even in the presence of loss, extremely flat band is obtainable, and the sign of the band still flips, which is consistent with our previous finding in a different system [5]. In general, it appears that the group velocity becomes independent of the loss when the losses of different subsystems are matched [5,16].

The system presented above satisfies the general criterion required to stop light [5]: the system is translationally invariant, and the width of one of the bands can be reversibly compressed to zero. Thus, the dynamic process in [5] can also be applied here to stop a light pulse. We start with large Δ, such that the middle band has a large bandwidth, and ω_A, ω_B are chosen such that this band can accommodate the incoming pulse, with each spectral component of the pulse occupying a unique wave vector [Fig. 2(a)]. After the pulse is completely in the system, we vary ω_A and ω_B until the bandwidth of the band is reduced to zero [Fig. 2(b)], at a rate slow compared with the frequency separation of the middle band from other bands.

We implement the system presented above in a photonic crystal of a square lattice of dielectric rods ($n = 3.5$) with a radius of $0.2a$ (a is the lattice constant) embedded in air ($n = 1$) (Fig. 3). The photonic crystal possesses a band gap for TM modes with electric field parallel to the rod axis. A single-mode waveguide is generated by removing one row of rods along the pulse propagation direction. Decreasing the radius of a rod to $0.1a$ and the dielectric
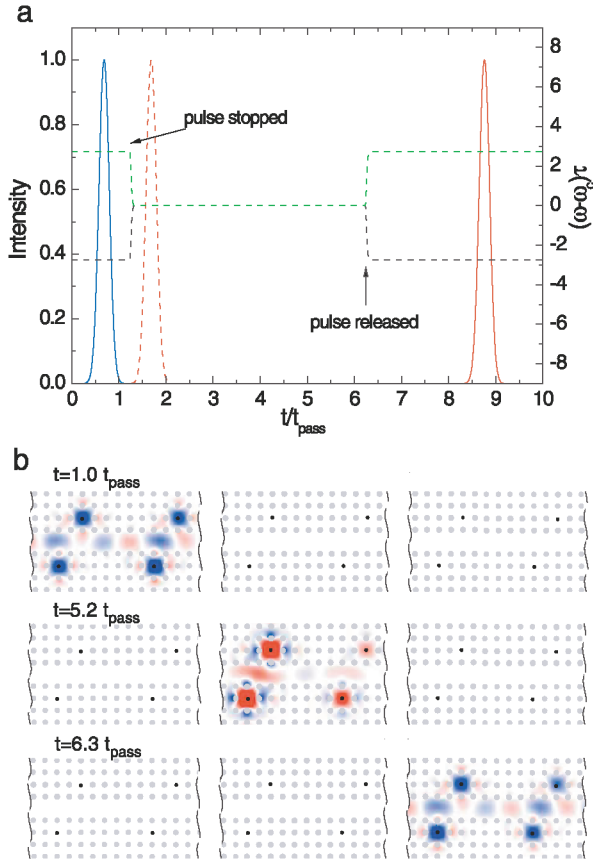
a

b

FIG. 3 (color). Propagation of an optical pulse through a waveguide-resonator complex in a photonic crystal system as the resonant frequencies of the cavities are varied. The photonic crystal consists of 100 cavity pairs. Fragments of the photonic crystal are shown in (b). The three fragments correspond to unit cells 12–13, 55–56, and 97–98. The dots indicate the positions of the dielectric rods. The black dots represent the cavities. (a) The dashed green and black lines represent the variation of ω_A and ω_B as a function of time, respectively. The blue solid line is the intensity of the incident pulse as recorded at the beginning of the waveguide. The red dashed and solid lines represent the intensity at the end of the waveguide, in the absence and the presence of modulation, respectively. (b) Snapshots of the electric field distributions in the photonic crystal at the indicated times. Red and blue represent large positive and negative electric fields, respectively. The same color scale is used for all the panels.

constant to $n = 2.24$ generates a single-mode cavity with resonance frequency at $\omega_c = 0.357(2\pi c/a)$. The nearest neighbor cavities are separated by a distance of $\ell_1 = 2a$ along the propagation direction, and the unit cell periodicity is $\ell = 8a$. The waveguide-cavity coupling occurs through a barrier of one rod, with a coupling rate of $1/\tau = \omega_c/235.8$. The resonant frequencies of the cavities are tuned by refractive index modulation of the cavity rods.

We simulate the entire process of stopping light for $N = 100$ pairs of cavities with the finite-difference-time-domain (FDTD) method [19], which solves Maxwell's equations without approximation. The computational cell

is truncated by uniaxial perfectly matched boundary layers [19]. Furthermore, we have used a large enough computational cell such that the result is free of any parasitic reflection from the right end of the computational boundary. The dynamic process for stopping light is shown in Fig. 3(a). We generate a Gaussian pulse in the waveguide (the process is independent of the pulse shape). The excitation reaches its peak at $t = 0.8t_{\mathrm{pass}}$, where t_{pass} is the traversal time of the pulse through the unmodulated waveguide. During the pulse generation, the cavities have a large frequency separation. The field is concentrated in both the waveguide and the cavities [Fig. 3(b), $t = 1.0t_{\mathrm{pass}}$], and the pulse propagates at a high speed of $v_g = 0.082\, c$. After the pulse is generated, we gradually reduce the frequency separation Δ to zero. During this process, the speed of light is first reduced to zero, and then its sign changes and the pulse starts propagating backwards slowly. (The sequence of the corresponding band structure is shown in Fig. 2.) As the bandwidth of the pulse is reduced, the field concentrates in the cavities [Fig. 3(b), $t = 5.2t_{\mathrm{pass}}$]. We use an index modulation with a form of $\exp[-t^2/\tau_{\mathrm{mod}}^2]$, where $\tau_{\mathrm{mod}} = 5\tau$. However, almost any modulation pattern and rate would satisfy adiabaticity in this system. When zero group velocity is reached, the photon pulse can be kept in the system as a stationary waveform for any time duration. In this simulation, we store the pulse for a time delay of $5.0t_{\mathrm{pass}}$, and then release the pulse by repeating the same index modulation in reverse [Fig. 3(b), $t = 6.3t_{\mathrm{pass}}$]. The pulse intensity as a function of time at the right end of the waveguide is plotted in Fig. 3(a), and shows the same temporal shape as both the pulse that propagates through the unmodulated system, and the initial pulse recorded at the left end of the waveguide. Thus, the pulse is perfectly recovered without distortion after the intended delay. In the FDTD simulations, we choose an index modulation of 1% and a modulation rate of 1.1 THz only to make the total simulation time feasible. The use of such extremely fast modulation demonstrates that the adiabaticity requirement in this system can be achieved easily. The simulation demonstrates a group velocity reduction to zero for a 4 ps pulse at the 1.55 μm wavelength.

Unlike the previously proposed scheme [5] based upon the band anticrossing mechanism, the structure proposed here has several important advantages, and, in fact, represents an optimal implementation of the general criterion.

(a) Only two resonators per unit cell are needed for the bandwidth to be compressed to absolute zero.

(b) The same system can be used for time reversal. The slope of the band can change sign as one modulates the resonant frequencies, which results in a time-reversal operation on the pulse [20].

(c) This system can operate with fast modulation rates while maintaining adiabaticity, which enables the use of the shortest waveguide. The total length of the waveguide L is determined by the initial bandwidth of the pulse,

which sets the maximum speed in the waveguide v_{g0}, and by the duration of the modulation τ_{mod}, which sets the distance that the pulse travels before it is stopped (i.e., $L \sim v_{g0}\tau_{\mathrm{pulse}} + v_{g0}\tau_{\mathrm{mod}}$, where τ_{pulse} is the length of the pulse). Because of the delay-bandwidth product, $v_{g0}\tau_{\mathrm{pulse}}$ is a constant independent of the signal bandwidth $\delta\omega$, and the length of the system can thus be estimated as $L \sim (10 + \delta\omega\tau_{\mathrm{mod}})l$. In this system, the gaps surrounding the middle band have sizes on the order of the cavity-waveguide coupling rate $1/\tau$, and are approximately independent of the slope of the middle band (Fig. 2). Thus, by *increasing* the waveguide coupling rate of the cavity, this gap can be made large, which enables the use of fast modulation while satisfying adiabaticity [5] and significantly reduces the length requirement of the structure. To accomplish the entire process of stopping and recovering a 100 ps pulse, for example, a waveguide with a length less than 30 microcavities modulated at a maximum speed of 20 GHz is sufficient.

(d) This system can compress the largest possible pulse bandwidth for a given refractive index modulation strength δn. For a resonance with frequency ω, the largest frequency shift possible for a given index modulation is about $\omega\delta n/n$. Therefore the largest compressible system bandwidth is approximately [5]

$$\delta\omega \simeq \omega\delta n/n, \qquad (6)$$

which sets the largest bandwidth of a pulse that can be stopped. The introduced system can achieve this optimal utilization of the system bandwidth. The dispersion over most of the bandwidth is small compared with a typical CROW band due to the existence of long-range through-waveguide coupling between the cavities. Such a reduction in dispersion is particularly prominent when the bandwidth is smaller than $1/\tau$. In the band structure of Fig. 2(a), since we used large index shifts to make FDTD simulations feasible, the band exhibits large dispersion. In practice, by operating in a regime where $\delta n \ll 1/\tau\omega_c$, the dispersion over most of the band is practically negligible. Furthermore, all dispersive effects scale with the second or higher orders of the system bandwidth, while the pulse delay ($\sim 1/v_g$) scales inversely with the system bandwidth. The dispersive effects integrated over time approach zero in the limit of the vanishing bandwidth. In this system, the presence of a zero-width band thus significantly reduces the effects of dispersion and also results in a more efficient utilization of the system bandwidth.

The all-optical EIT-like system represents a dramatic improvement over the atomic-electronic schemes for stopping light. For a small refractive index shift of $\delta n/n = 10^{-4}$ achievable in practical optoelectronic devices [21], and assuming a carrier frequency of approximately 200 THz, as used in optical communications, the achievable bandwidths are on the order of 20 GHz, which is comparable to the bandwidth of a single wavelength channel in high-speed optical systems. In comparison, the atomic stop light schemes have experimentally demonstrated bandwidths less than 100 kHz [7,8,22,23]. The all-optical storage times are limited only by the cavity lifetimes, which are approaching millisecond time scales [24,25]. The on-chip and room temperature operation of all-optical schemes may thus enable completely new classical and quantum information processing capabilities.

*Electronic address: shanhui@stanford.edu

[1] R. Ramaswami and K. N. Sivarajan, *Optical Networks: A Practical Perspective* (Morgan Kaufmann, San Francisco, CA, 1998).

[2] M. D. Lukin and A. Imamoglu, Nature (London) **413**, 273 (2001).

[3] L. M. Duan, M. D. Lukin, J. I. Cirac, and P. Zoller, Nature (London) **414**, 413 (2001).

[4] M. Fleischhauer and M. D. Lukin, Phys. Rev. A **65**, 022314 (2002).

[5] M. F. Yanik and S. Fan, Phys. Rev. Lett. **92**, 083901 (2004).

[6] M. D. Lukin, S. F. Yelin, and M. Fleischhauer, Phys. Rev. Lett. **84**, 4232 (2000).

[7] C. Liu, Z. Dutton, C. H. Behroozi, and L. V. Hau, Nature (London) **409**, 490 (2001).

[8] D. F. Phillips, A. Fleischhauer, A. Mair, R. L. Walsworth, and M. D. Lukin, Phys. Rev. Lett. **86**, 783 (2001).

[9] S. E. Harris, Phys. Rev. Lett. **77**, 5357 (1996).

[10] A. G. Litvak and M. D. Tokman, Phys. Rev. Lett. **88**, 095003 (2002).

[11] D. D. Smith, H. Chang, K. A. Fuller, A. T. Rosenberger, and R. W. Boyd, Phys. Rev. A **69**, 063804 (2004).

[12] L. Maleki, A. B. Matsho, A. A. Savchenkov, and V. S. Ilchenko, Opt. Lett. **29**, 626 (2004).

[13] W. Suh, Z. Wang, and S. Fan, IEEE J. Quantum Electron. **40**, 1511 (2004).

[14] G. Lenz, B. J. Eggleton, C. K. Madsen, and R. E. Slusher, IEEE J. Quantum Electron. **37**, 525 (2001).

[15] Z. Wang and S. Fan, Phys. Rev. E **68**, 066616 (2003).

[16] M. F. Yanik and S. Fan, Phys. Rev. A (to be published).

[17] S. Fan *et al.*, Phys. Rev. B **59**, 15882 (1999).

[18] G. Juzeliunas and H. J. Carmichael, Phys. Rev. A **65**, 021601R (2002).

[19] A. Taflove and S. C. Hagness, *Computational Electrodynamics* (Artech House, Norwood, MA, 2000).

[20] M. F. Yanik and S. Fan, Phys. Rev. Lett. **93**, 173903 (2004).

[21] S. L. Chuang, *Physics of Optoelectronic Devices* (Interscience, New York, 1995).

[22] A. V. Turukhin *et al.*, Phys. Rev. Lett. **88**, 023602 (2002).

[23] M. S. Bigelow, N. N. Lepeshkin, and R. W. Boyd, Phys. Rev. Lett. **90**, 113903 (2003).

[24] D. W. Vernooy, V. S. Ilchenko, H. Mabuchi, E. W. Streed, and H. J. Kimble, Opt. Lett. **23**, 247 (1998).

[25] K. Vahala, *Optical Microcavities* (World Scientific Publishing, Hackensack, NJ, 2004).